Aerosol and Air Quality Research, 11: 80–89, 2011

ISSN: 1680-8584 print / 2071-1409 online
doi: 10.4209/aaqr.2010.11.0095

Characteristics of Submicron-sized Aerosol Filtration and Pressure Drop of an Electret Filter Installed in an Air Diffuser in a Residential Apartment Unit

Kwang-Chul Noh[1], Jae-Hong Park[1], Yee-Kyeong Jung[2], Sunghwan Yi[3], Jungho Hwang[1*]

[1] *Department of Mechanical Engineering, Yonsei University, Seoul 120-749, Korea*
[2] *Refrigerator R&D Center, Daewoo Electronics Corp., 412-2 Cheongcheon-dong, Bupyeong-Gu, Incheon 403-302, Korea*
[3] *Ventopia Ltd., 108 Haenglim bldg., Tonui-dong, Jongno-Gu, Seoul 110-808, Korea*

ABSTRACT

We investigated submicron-sized aerosol filtration and the pressure drop of an electret filter called a "Flimmer filter." The fibers of the filter are aligned parallel to the direction of the airflow, unlike conventional fibrous filters or conventional electret filters. Lab-scale tests were performed first in a laboratory duct system for submicron particle removal efficiency and pressure drop of the filter. Then, Field tests were conducted in an apartment home using two portable aerosol spectrometers and with a Flimmer filter installed at the terminal of a duct within a mechanical ventilation system. The removal efficiencies at the face velocity of 1.0 m/s for 0.4 μm and 0.6 μm were 52% and 65%, respectively. The removal efficiency for $PM_{1.0}$ was about 51%. Through an adapted mass balance model, indoor particle concentrations both in number and mass were predicted. The predicted results for the temporal variations of 0.4 and 0.6 μm sized particle, and $PM_{1.0}$ correlated well with the results obtained from the field tests. When the face velocity was 1.0 m/s, which is the nominal operating condition of the test filter, the pressure drop was 11.5 Pa, which is relatively lower than the pressure drops of other conventional fibrous filters or conventional electret filters having the same filtration efficiency.

Keywords: Electret filter; Filtration; Pressure drop; Ventilation.

INTRODUCTION

The particle collection efficiency and pressure loss of a filter depend on structural aspects of the filter (e.g. porosity, fiber diameter, and filter thickness), operational conditions (e.g. face velocity, temperature, and relative humidity), and particle characteristics (e.g. density, size, and phase) (Hinds, 1999; Liu *et al*., 2003; Huang *et al*., 2007; Shin *et al*., 2008; Kim *et al*., 2010; Tekasakul *et al*., 2010). As the needs for smaller energy consumption and higher indoor air quality in buildings are increasing, the performance of a filter (e.g. pressure drop and collection efficiency) has gradually been important (Bakö *et al*., 2008; Zuraimi and Tham, 2009; Kim *et al*., 2010; Noh and Hwang, 2010). Conventional ventilation filters are located inside heating, ventilation, and air conditioning (HVAC) systems, or total heat exchangers, within housing units. Filters are exposed to air supplied from the outside environment and air recirculated from the indoor environment.

Electret filters are deep-bed fibrous filters used in air filtration composed of high-porosity, coarse fibers, which allow for low flow resistance. Since the fibers are charged, electrical forces act between the fibers and any existing particles (Emi *et al*., 1987). The particle capture characteristics of electret filters rely on a combination of conventional mechanical mechanisms (i.e. impaction, interception, and diffusion) and electrostatic mechanisms. If the particles are charged, an enhanced Coulombic force will also affect particle capture. In general, the collection efficiency of an electret filter is higher than that of a conventional fibrous filter, particularly for submicron-sized particles (Emi *et al*., 1987; Hanley *et al*., 1999). However, the non-uniformity of the charging and the decay of surface charge density with time under normal operating conditions are two drawbacks of existing electret filter technologies. Many researches were conducted in order to identify the characteristics of electret filter media. Hanley *et al*. (1999) studied the effect of loading dust type on the filtration efficiency of electet filters. Their results showed that all the ambient and in-home exposed filters had substantial decreases in filtration efficiency with loading but laboratory tests often produced either little change or increases with loading rather than decreases. Romay *et al*. (1998) presented experimental data on the performance of three types of commercially available fibrous electret filters. They showed that the experimentally

* Corresponding author. Tel: 82-2-2123-2821;
Fax: 82-2-312-2821
E-mail address: hwangjh@yonsei.ac.kr

obtained power law exponents were in good agreement with those predicted by previous theory. Kim *et al*. (2007) studied nanoparticle penetration through commercial electret filter media using silver nano particles from 3 nm to 20 nm at three different face velocities in order to define nano particle filtration characteristics of commercial fibrous filter media. The results showed a very high uniformity with small error bars for all filter media tested and the particle penetration decreased continuously down to 3 nm as expected from the classical filtration theory. Podgórski and Bałazy (2008) proposed a numerical method for determining deposition efficiency for naturally charged submicron particles within bipolarly charged fibrous filters. They reported that a good agreement between the results of Brownian dynamics calculations and their experimental data was obtained. Ji *et al*. (2003) studied the effect of particle loading on the collection performance of an electret cabin air filter. They showed that the collection efficiency of the electret filter media degraded as more particles were loaded and the electret filter media captured the highly charged particles more efficiently.

The "Flimmer filter," which is a type of electret filter, was developed by a Swedish company (Fresh AB) and has been used in a few nations as a component of a natural ventilation system. The fibers of a Flimmer filter are mostly dispersed toward the airflow direction, as shown in Fig. 1(a), in contrast to a conventional fibrous filter or a conventional electret filter, in which the longitudinal axes of the fibers are typically perpendicular to the airflow, as shown in Fig. 1(b). Recently, a type of Flimmer filter has been applied to the mechanical ventilation and air-conditioning system in a subway station by Li and Jo (2010). They reported that the filtration quality of the filter was higher than the mechanical filter or the general panel-type electret filter with a small drop in pressure drop even at a high filtration velocity. However, the Flimmer filter has not been used as a component of mechanical ventilation filter in a residential apartment unit until now.

Most of micron particles are intercepted by the hairs of the nostril but submicron particles can reach the lung and deposit in the alveoli (Madl and Pinkerson, 2009). In this study, the measurement of submicron particle removal efficiency and pressure drop of a Flimmer filter were performed first in a laboratory duct system under varying operating conditions. Then, field tests were performed with a Flimmer filter installed at the terminal of a duct, i.e. upstream of an air diffuser of a mechanical ventilation

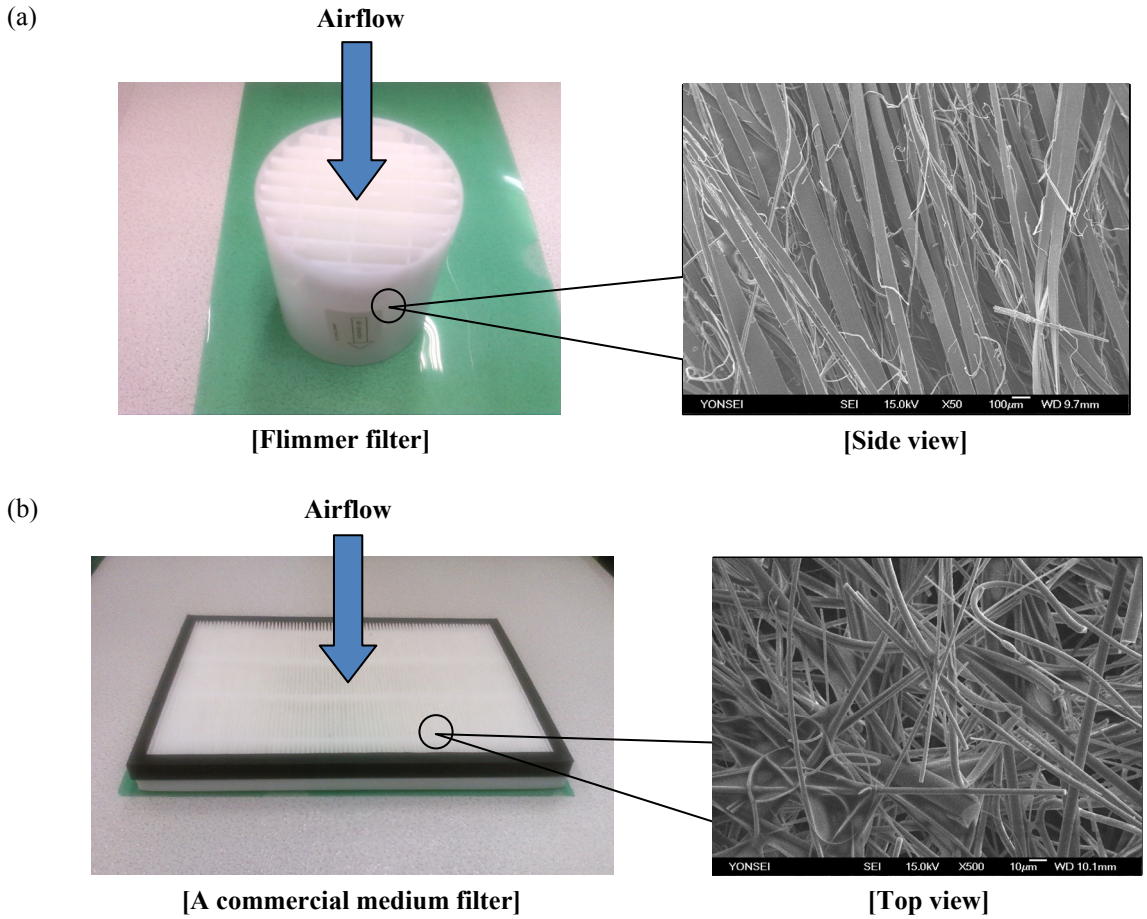

Fig. 1. Comparison of a conventional filter and Flimmer filter. (a) Photo and SEM images of Flimmer filter; airflow is parallel to fibers of filter; (b) Photo and SEM images of a conventional medium filter; airflow is perpendicular to fibers of filter.

system, in a residential apartment unit. Through an adapted mass balance model, indoor particle concentrations both in number and mass were predicted and compared to the experimental results. The decrease in filtration performance as particles were loaded in the filter was not considered.

EXPERIMENTS

The removal efficiency for submicron particle and the pressure drop of the Flimmer filter were investigated first in a laboratory duct system. Then, the performance of the Flimmer filter was tested in the field.

Test Filter

The test filter system was composed of a filter with polypropylene fibers and a housing component as shown in Fig. 1(a). Within the test filter, particles are separated from the air stream along the length of the fibers. The inner diameter of the filter housing was 90 mm and the fiber length was 70mm. Fig. 1(a) also shows the SEM (scanning electron microscope) image for the polypropylene fibers. The diameters of the polypropylene fibers were in the range of 1 to 100 μm and the average diameter was approximately 50 μm. The solidity of the filter, which is defined as the ratio of fiber volume to total one, was measured as approximately 0.0135 using a measuring cylinder. The filter was placed in a cylinder of a known volume of some liquid and the volume change due to the filter was measured.

The filter fibers have an electrically charged layer that is fitted under the surface of the filter fiber. The surface charge density of the test filter was measured with an electrostatic probe and an electrostatic voltmeter (Monroe Electronics, Model 244). The schematic of measurements is shown in Fig. 2. The distance between the surface of fibres and the probe, 3mm, was selected as the test condition for accuracy. The capacity C (F) of a fiber sample that carries a charge Q (Coulomb) with a surface area A (m^2) and a thickness d (m), can be expressed as (Tabti *et al*., 2009):

$$C = \frac{Q}{A} = \frac{\varepsilon \cdot V}{d} \tag{1}$$

where V is the surface potential (Volt) measured in volts, and ε is the dielectric constant for air (8.85×10^{-12} F/m). The surface potential was measured within the range of 1.36 to 2.71 kV. From Eq. (1), the surface charge density was calculated to be within the range of 12 to 24 μC/m^2. The average and the standard deviation were 16.3 μC/m^2 and 3.56 μC/m^2, respectively. These values were similar to surface charge densities of other commercial electret filters (i.e. 10–45 μC/m^2 in the case of polypropylene made by a melt-blown method, Nifuku *et al*., 2001).

Lab-scale Test

A schematic of the laboratory-scale experimental system for testing the performance of a Flimmer filter is shown in Fig. 3. The lab-scale test system consisted of a test duct, a particle generation system, and a measurement system. The test duct was made of acryl, and its outer diameter and length were 0.1 m and 1 m, respectively. During the experiments, the temperature and relative humidity in the test laboratory using multi-function measuring instrument (Testo, 435-3) were 21 ± 1°C and 50 ± 10%, respectively. The accuracies of temperature and relative humidity were within ± 0.5°C and ± 2.5%, respectively.

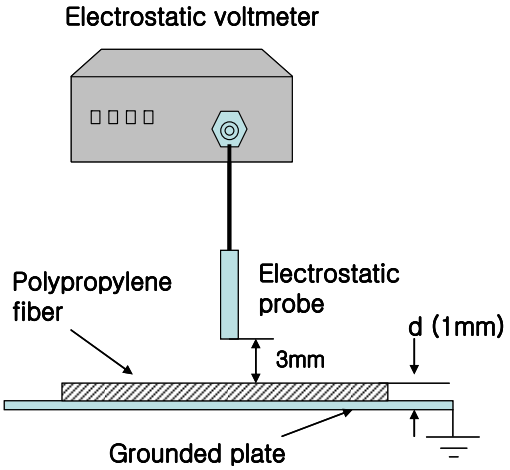

Fig. 2. Experimental set-up for the measurement of surface charge density.

Potassium chloride (KCl) particles were used as test particles. A cloud of particle-free, compressed air from a clean air supply system consisting of an oil trap, a diffusion dryer and a High Efficiency Particulate Air (HEPA) filter was delivered to a Collison-type atomizer with a solution containing KCl. The test particles from the atomizer passed through a diffusion dryer for water removal followed by a neutralizer (HCT, Soft X-ray charger 4530), which neutralizes particles until the electrostatic charge reaches the Boltzmann charge equilibrium. The desired concentrations of the test particles were controlled by using a laminar flow meter (LFM). Fig. 4 shows the size distribution of KCl particles. The size distribution was measured at the sampling port 1 in Fig. 3 when the velocity was 0.5 m/s. The particle concentrations were measured with a scanning mobility particle sizer (SMPS; TSI, model 3936). The SMPS consisted of a classifier controller (TSI, 3080), differential mobility analyzer (DMA; TSI, 3081), condensation particle counter (CPC; TSI, 3022A), and a neutralizer (HCT, Soft X-ray charger 4530) with a sampling airflow rate of 0.3 L/min. The SMPS was controlled to measure particles from 0.019 to 0.604 μm with a mobility equivalent diameter. For a KCl aqueous solution of 10%, the total concentration of the KCl aerosol particles was about 2×10^4 particles per cubic centimeter and the geometric mean diameter was 0.1 μm. The KCl solution provided particle distributions that are somewhat reflective of indoor environments (Owen and Ensor, 1990; Hussein *et al*., 2006).

The face velocities upstream of the filter, which were measured with a flow anemometer (PROVA, model AVM07), were controlled with a fan controller and set to

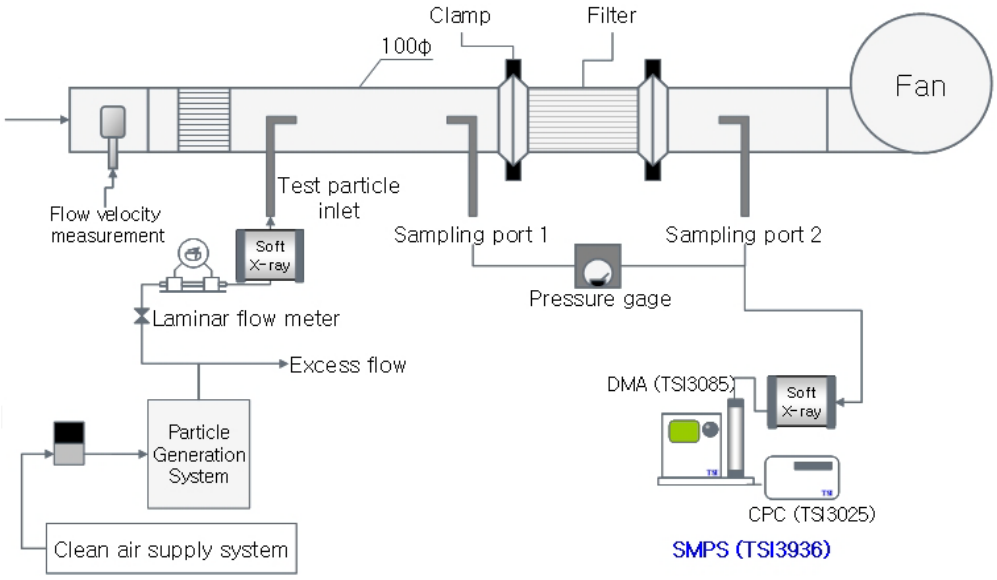

Fig. 3. Schematic of the experimental system for testing the performance of a Flimmer filter.

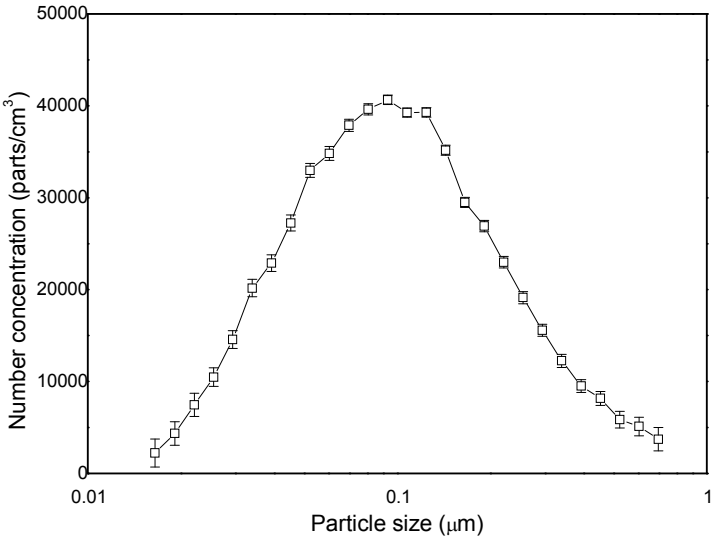

Fig. 4. Size distribution of test particles upstream of the filter.

0.5, 1.0, 1.5, and 2.0 m/s. The values for the face velocities were chosen in accordance to the nominal operating airflow rate of the Flimmer filter, which was determined to be 25 m^3/h (about 1.0 m/s of face velocity). The filter was installed in the middle of the test duct. Two sampling probes, made of 6.5 mm stainless steel, were located at the front and back of the filter for measuring pressure drop and aerosol concentration. The pressure drop across the electret filter was monitored by multi-function measuring instrument (Testo, 435-3) during the test period.

The particle concentrations were measured with the SMPS. The fractional (size-resolved) particle collection efficiency, $\eta(d_p)$, of the filter based on particle number is defined as follows:

$$\eta(d_p) = 1 - \frac{C_{down}(d_p)}{C_{up}(d_p)} \quad (2)$$

where, $C_{up}(d_p)$ and $C_{down}(d_p)$ represent the aerosol number concentrations (#/cm^3) with size d_p, measured upstream and downstream of the filter, respectively. d_p is the mobility equivalent diameter (μm).

Assuming a spherical shape and particle density, the mass concentration with size d_p, is determined by multiplying the particle mass by measured number concentration. The overall collection efficiency of airborne particles of filter based on particle mass then becomes,

$$\eta_{overall} = \frac{\int \eta(d_p) C_{up}(d_p) \cdot d_p^{\,3} dd_p}{\int C_{up}(d_p) \cdot d_p^{\,3} dd_p} = 1 - \frac{M_{down}}{M_{up}} \quad (3)$$

where, M_{up} and M_{down} represent the total aerosol mass concentrations (g/cm^3) upstream and downstream of the filter, respectively.

Field Test

Field tests were performed in an unfurnished apartment room. Fig. 5 shows the schematics of the test room and ventilation apparatuses used for the field tests. The test room within the apartment home is 3.5 meters in length, 4.5 meters wide and 2.3 meters in height. The mechanical ventilation system was composed of a supply diffuser, an exhaust diffuser, a filter, a heat exchanger and two fans. The test filter was installed in the supply diffuser. The fraction of outdoor air supply was 100%. A Flimmer filter was installed upstream of the supply diffuser. The ambient particle number and mass concentrations were measured inside and outside the room with two portable aerosol spectrometers (Grimm, model 1.109) at a sampling airflow rate of 1.2 L/min. It can detect airborne aerosol particles from 0.25 to 32 μm of optical equivalent diameter by using a form of light scattering detection. During the field tests, the ambient temperature and relative humidity were 10 ± 3.0°C and 57 ± 5%, respectively. The temperature and the relative humidity in the apartment were 20 ± 1.0°C and 30 ± 5%, respectively.

MODELLING

The indoor particle concentration in a space can be predicted with a mass balance model. The model consists of source and loss terms. When particles are not generated indoors, the indoor particle concentration is reduced with ventilation and finally achieves a steady-state condition. When the indoor space is well-mixed and the outdoor particle concentration is relatively constant, the temporal variations of indoor particle number concentration at a certain size can be predicted using the fractional particle collection efficiency in Eq. (2) and the following number balance equation,

$$V\frac{dC_{in}(d_p)}{dt} = C_{out}(d_p)\left[\dot{Q}_V(1-\eta(d_p)) + \dot{Q}_I \cdot P(d_p)\right] - C_{in}(d_p)\left[k(d_p)\cdot V + \dot{Q}_V + \dot{Q}_I\right] \quad (4)$$

where, $\dot{Q}_V$ is the ventilation rate of the test room (m^3/h), $k(d_p)$ is the deposition rate at a particle size ($1/h^{-1}$), V is the volume of the test room (m^3), $\dot{Q}_I$ is the air infiltration rate (m^3/h), $C_{in}(d_p)$ is the indoor concentration for each particle size (parts/m^3), $C_{out}(d_p)$ is the outdoor concentration for each particle size (parts/m^3), and $P(d_p)$ is a dimensionless quantity representing the penetration efficiency at a particle size (dimensionless).

Similarly, the temporal variations of total mass of particles can be predicted using the mass balance equation. The mass balance equation for $PM_{1.0}$ becomes,

$$V\frac{dM_{in}}{dt} = M_{out}\left[\dot{Q}_V(1-\eta_{PM1.0}) + \dot{Q}_I \cdot P_{PM1.0}\right] - M_{in}\left[k_{PM1.0}\cdot V + \dot{Q}_V + \dot{Q}_I\right] \quad (5)$$

where, M_{in} and M_{out} are the total indoor and outdoor mass concentrations of $PM_{1.0}$ (g/cm^3), respectively. $\eta_{PM1.0}$ is the $\eta_{overall}$ for $PM_{1.0}$. $P_{PM1.0}$ is the penetration efficiency of $PM_{1.0}$ and $k_{PM1.0}$ is the deposition rate of $PM_{1.0}$ (h^{-1}). Assuming no indoor sources or no ventilation system running, they are defined as,

$$P_{PM1.0} = \frac{M_{in}(d_p \le 1.0\mu m)}{M_{out}(d_p \le 1.0\mu m)} = \frac{\sum_{d_p=0}^{1.0} P(d_p)\cdot C_{out}(d_p)\cdot {d_p}^3}{\sum_{d_p=0}^{1.0} C_{out}(d_p)\cdot {d_p}^3} \quad (6)$$

$$k_{PM1.0} = Average\ value\ of\ \frac{d}{dt}\left(\frac{\sum_{d_p=0}^{1.0} k(d_p)\cdot C_{in}(d_p)\cdot {d_p}^3}{\sum_{d_p=0}^{1.0} C_{in}(d_p)\cdot {d_p}^3}\right) \quad (7)$$

where, *dt* is the time interval.

The temporal variations of individual particle concentration and total particle mass indoors were predicted using Eqs. (4)–(7), and subsequently compared to the experimental counterparts.

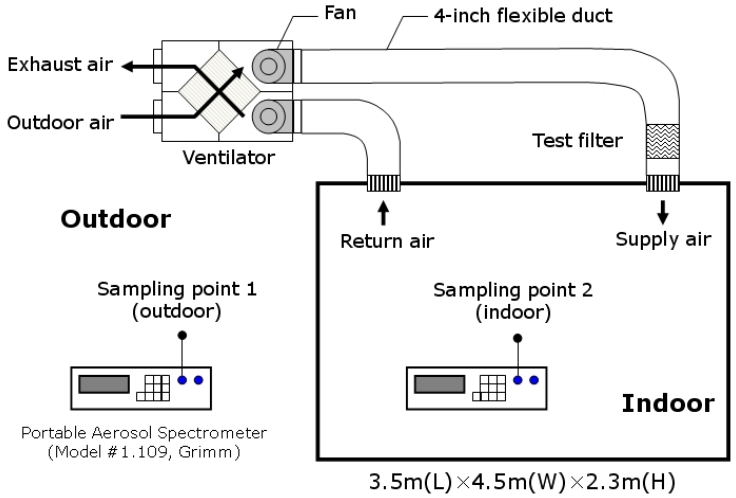

Fig. 5. Schematic of the room and ventilation apparatuses for field tests.

RESULTS AND DISCUSSION

Lab-scale Test for Pressure Drop and Particle Removal

The relationship between the pressure drop and the face velocity for the clean filter media was obtained, as shown in Fig. 6(a). This figure shows that the pressure drop was a quadratic function of face velocity. When the velocity was 1.0 m/s, the corresponding pressure drop was 11.5 Pa. When the velocity was 2.0 m/s, the pressure drop was about 30.0 Pa. The experimental data were compared to calculated results using various pressure drop models suggested in previous studies (Kimura and Iinoya, 1959; KACA, 2007). The summaries of those models are presented in Table 1. For calculations, the average diameter of the fibers was assumed as 50 μm (d_f) and the solidity of the filter (α) as 0.0135. The previous semi-empirical or theoretical models predicted pressure drops higher than the experimental results under the same conditions. This deviation is likely due to the fact that pressure drop models were derived for fibrous filters in which the fibers are perpendicular to the airflow direction, in contrast to the test electret filter. The results imply that higher airflow rates can be obtained at lower pressure drops, which may have an energy saving impact when the Flimmer filter is used as the ventilation filter.

The average fractional collection efficiencies of clean filter media subjected to neutralized KCl particles are shown in Fig. 6(b) for varying face velocities. The experiments for evaluating the collection efficiency were carried out over 5 times under the same conditions. The maximum error did not exceed by 4%. For a given face velocity, the collection efficiency generally increased with

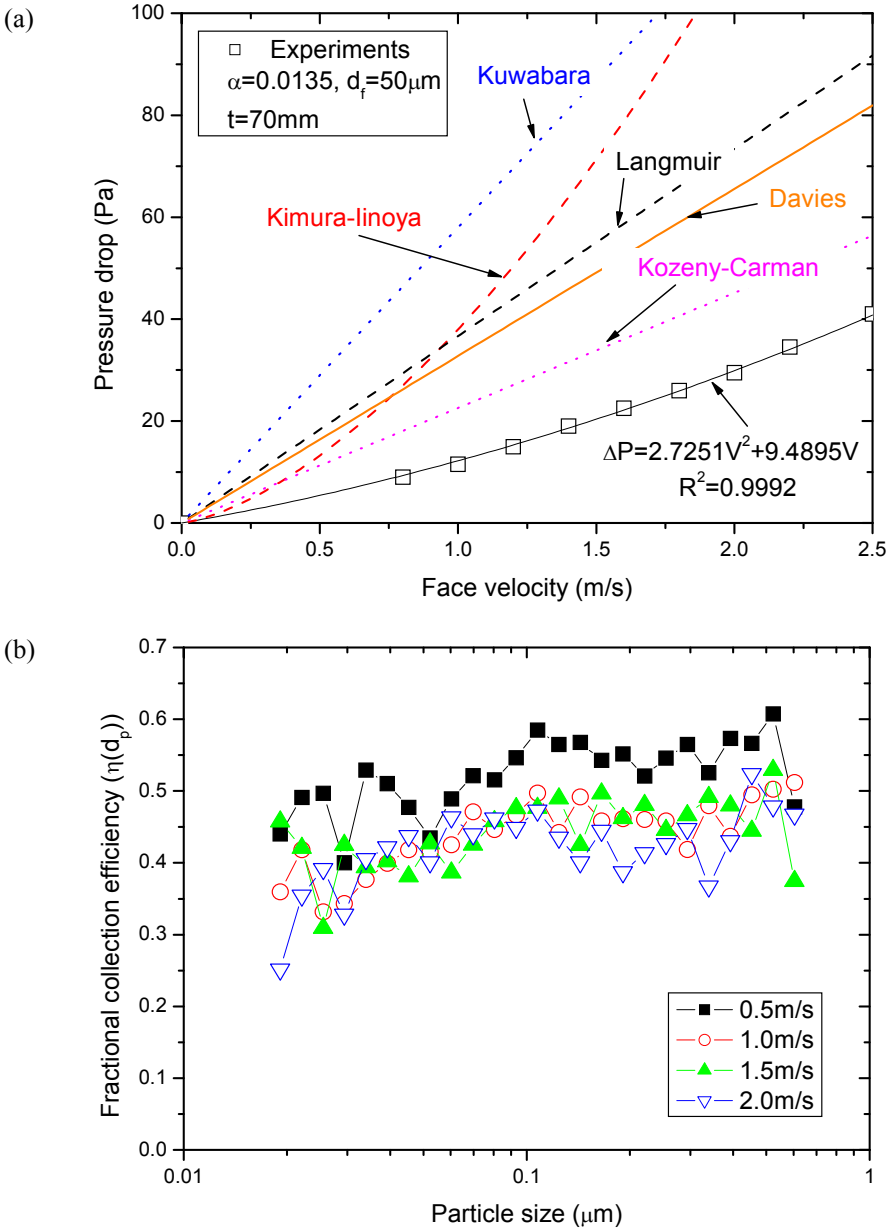

Fig. 6. Pressure drop and collection efficiency in the lab-scale test. (a) Pressure drop; (b) Collection efficiency.

Table 1. Different pressure drop models of filters suggested in the previous studies.

Pressure drop (Pa)	$\Delta P = C_D \cdot \left(\frac{2\rho U_0^2}{\pi}\right) \times \left(\frac{\alpha}{1-\alpha}\right) \times \left(\frac{t}{d_f}\right)$	
Researcher	Drag coefficient, C_D	Remark
Kozeny-Carman	$\frac{8\pi k_1}{\mathrm{Re}} \cdot \frac{\alpha}{(1-\alpha)^2}$	Semi-empirical, $k_1 = f(\alpha)$, $\mathrm{Re} \le 1$
Langmuir	$\frac{11.2\pi}{\mathrm{Re}} \cdot \frac{1}{-\ln\alpha + 2\alpha - \alpha^2/2 - 3/2}$	Semi-empirical, $\mathrm{Re} \le 1$
Davies	$\frac{32\pi}{\mathrm{Re}} \cdot \alpha^{0.5}\left(1 + 56\alpha^2\right)$	Empirical, $0.006 < \alpha < 0.3$, $\mathrm{Re} \le 1$
Kuwabara	$\frac{16\pi}{\mathrm{Re}} \cdot \frac{1}{-\ln\alpha + 2\alpha - \alpha^2/2 - 3/2}$	Theoretical, $\mathrm{Re} \le 1$
Kimura-Iinoya	$0.6 + \frac{4.7}{\sqrt{\mathrm{Re}}} + \frac{1.1}{\mathrm{Re}}$	Empirical, $10^{-3} < \mathrm{Re} < 10^2$, $3 < d_f < 270$ μm

where, α: solidity of filter, ρ: air density (kg/m^3), U_0: face velocity (m/s), t: length of filter (m), d_f: diameter of fiber (m), Re: Reynolds number ($= \frac{\rho U d_f}{\mu}$), U: media velocity ($= \frac{U_0}{1-\alpha}$, m/s), μ: viscosity (kg/m·s), $k_1 = 27$ (in our case)

particle size. For a given particle size, the collection efficiency generally decreased with face velocity. However, the collection efficiency displayed little change for velocities greater than 1.0 m/s. The collection efficiency at 0.5 m/s was in the range of 40–60%. When the face velocity was 1.0 m/s, the collection efficiencies for all tested particle sizes were reduced by approximately 10%, as compared to those at 0.5 m/s. When the face velocity increased to 1.5 m/s or 2.0 m/s, the collection efficiency did not experience further reductions. As the face velocity increases, the collection efficiency due to interception does not change at a particle size (Hinds, 1999). The collection efficiency due to diffusion and electrostatic force also little changes when the face velocity is over a certain value (Fjeld and Owens, 1988; Hinds, 1999). Consequently, the collection efficiency for submicron particles remains constant when the face velocity is over a certain value; which explains why there was little change in the collection efficiency for submicron particles for a face velocity of 1.0–2.0 m/s, as shown in Fig. 6(b).

The mass-based particle removal efficiencies of clean filter media were calculated from the SMPS data for face velocities varying from 0.5 to 2.0 m/s. Test particles were assumed to be spheres with a bulk density of 1.984 g/cm^3. Table 2 summarizes mass-based particle removal efficiencies for particles having the number concentration distribution shown in Fig. 4. As the face velocity increased, the PM removal efficiency was gradually reduced.

Table 2. Mass-based removal efficiency for particles of number concentration distribution shown in Fig. 4.

Face velocity (m/s)	0.5	1.0	1.5	2.0
Removal efficiency (%)	55 ± 1	48 ± 1	46 ± 2	4 5± 2

Field Test for Outdoor Particle Removal

Fig. 7 shows the number distribution of outdoor particles during the field tests. The tests were performed 5 times inside and outside the apartment during two days. The sampling interval for particle concentration was 1 minute. Average values are plotted, and the deviation was 10% overall. The temporal variations of indoor particle concentrations (both in number and mass) were predicted by solving Eqs. (5) and (6), and later compared to the experimental results in Fig. 8. The initial condition of indoor particle concentration was controlled to be the same as the outdoor particle distribution by means of opening the windows. In prediction, the infiltration rate was assumed to be 0.4/h for the calculations. In this study, the penetration efficiencies and the deposition rates for particle size, estimated by Long *et al*. (2001), were used for the calculations (see Table 3), since their study was also based on no indoor source. They measured air exchange rates and concentrations of indoor and outdoor particles at night. Then, it was assumed in their study that there were negligible particle sources at indoor and outdoor. The data of air exchange rates and average indoor and outdoor particle concentrations were used in a physical-statistical model based on the indoor air mass balance equation to estimate penetration efficiencies and deposition rates (Long *et al*., 2001). The mechanical ventilation airflow rate was measured about 25 m^3/h using an air capture hood (KNS-233, Kona Sapporo Ltd., Japan), and the face velocity upstream of filter was about 1.0 m/s.

Fig. 8(a) shows that as experimental time continued, the indoor particle concentration decreased since a particle generation source did not exist indoors. The time it took to reach the steady-state condition was approximately 3 hours. Two particle sizes of 0.4 and 0.6 μm were chosen to compare the field tests and lab ones. The predicted results for 0.4 and 0.6 μm sized particles agreed with the

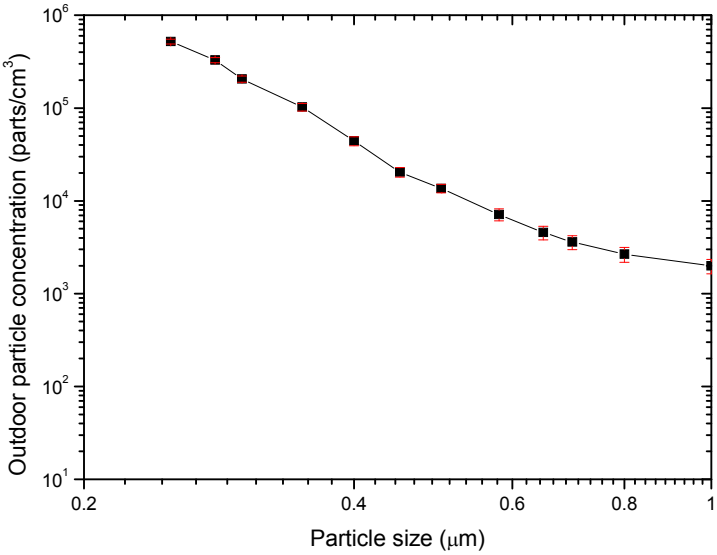

Fig. 7. Outdoor particle concentration distribution during the field tests.

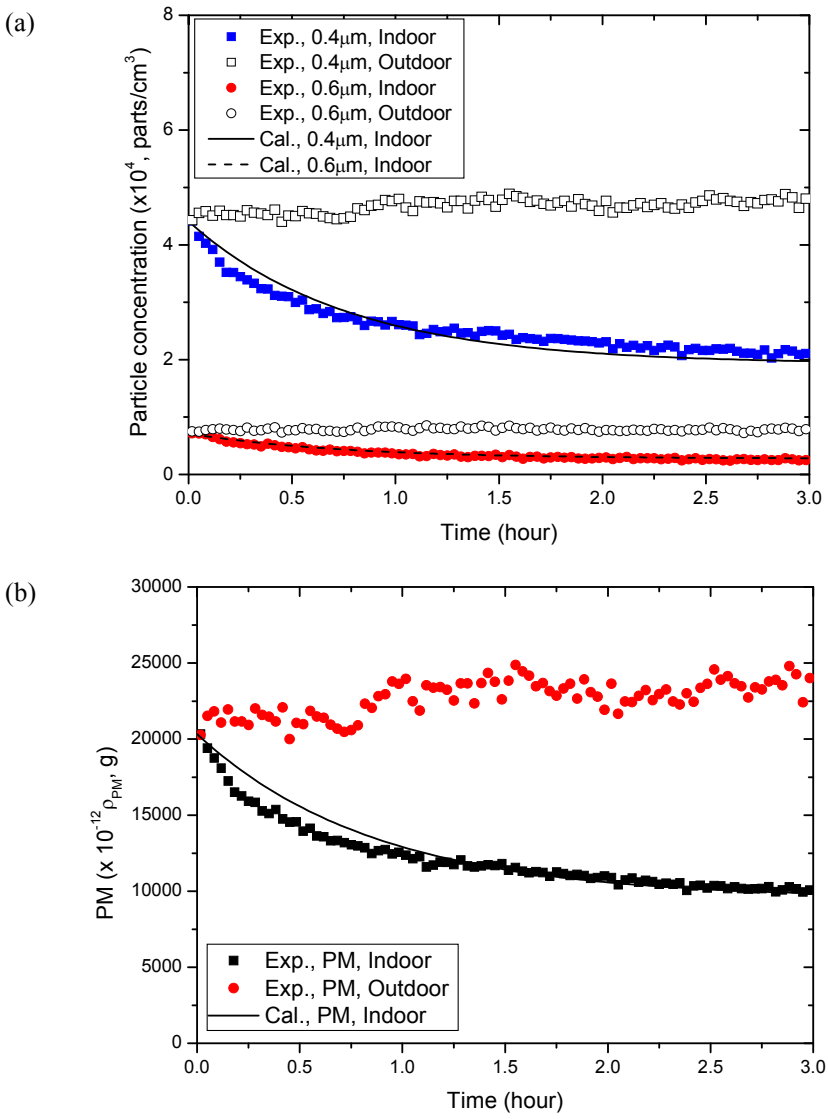

Fig. 8. Comparison of experimental and calculated data for temporal variations of indoor particle concentrations. (a) Number concentrations of 0.4 and 0.6 μm particles; (b) Mass concentration of $PM_{1.0}$.

Table 3. Penetration efficiency ($P(d_p)$) and particle deposition rate ($k(d_p)$) when the windows and door was closed (Long *et al*., 2001).

Size interval (μm)	Penetration efficiency	Deposition rate (1/h)
0.2–0.3	0.80	0.19
0.3–0.4	0.78	0.23
0.4–0.5	0.74	0.22
0.7–1.0	0.66	0.35

experimental results within 10% of error. The removal efficiencies for 0.4 μm and 0.6 μm were 52% and 65%, respectively, for a face velocity of 1.0 m/s.

Fig. 8(b) shows the temporal variations of indoor $PM_{1.0}$. The penetration efficiency and the deposition rate for $PM_{1.0}$ were calculated using Eqs. (6) and (7) along with the outdoor particle distribution. In calculation, the values of P and k for individual particle size were taken from the literature (Long *et al*., 2001). The calculated values from Eqs. (6) and (7) were 0.77 (dimensionless) and 0.222 (1/h), respectively. The predicted decay result for $PM_{1.0}$ correlated well with the experimental result. When the indoor particle concentration reached the steady-state condition, the removal efficiency for $PM_{1.0}$ was about 51%.

CONCLUSIONS

Characteristics of submicron-sized aerosol filtration and pressure drop of an electret filter were investigated in this study. The "Flimmer filter" is a type of electret filter in which its fibers are aligned parallel to the airflow direction, contrary to conventional fibrous filters. Lab-scale tests were performed first in a laboratory duct system for submicron particle removal efficiency and pressure drop of the filter. Then, Fields tests were conducted in an apartment.

The pressure drop of the test filter was a quadratic function of face velocity. When the face velocity was 1.0 m/s, the pressure drop was 11.5 Pa, which is relatively lower than the pressure drops of the conventional fibrous filters or electret filters having the similar filtration performance. Therefore, the Flimmer filter installed at the terminal of a duct operating within a mechanical ventilation system in a housing unit performs better than the conventional filter under the same conditions in regards to saving energy. In field test, the removal efficiencies at 1.0 m/s, a nominal operating condition of the filter, for 0.4 μm and 0.6 μm were about 52% and 65%, respectively. The removal efficiency for $PM_{1.0}$ was about 51%. The indoor particle concentration in a space was predicted with a number and a mass balance models. In prediction, the penetration efficiency and the deposition rate of PM were newly derived for the purpose of predicting the temporal variation of indoor particle mass concentrations. The predicted results for the temporal variations of 0.4 and 0.6 μm sized particles and $PM_{1.0}$ correlated well with the results obtained from field tests within 10% of error.

ACKNOWLEDGMENTS

This research was supported by a grant (06ConstructionCoreB02) from High-tech Urban Development Program (HUDP) funded by Ministry of Land, Transport, and Maritime Affairs of Korea Government.

REFERENCES

Bakö, G., Clausen, G. and Weshler, C.J. (2008). Is the Use of Particle Filtration Justified? Costs and Benefits of Filtration with Respect to Health Effects, Building Cleaning and Occupant Productivity. *Build. Environ*. 43: 1647–1657.

Emi, H., Kanaoka, C., Otani, Y. and Ishiguro, T. (1987). Collection Mechanisms of Electret Filter. *Part. Sci. Technol.* 5: 161–171.

Fjeld, R.A. and Owens, T.M. (1988). The Effect of Particle Charge on Penetration in an Electret Filter. *IEEE Trans. Ind. Appl.* 24: 725–731.

Hanley, J.T., Ensor, D.S., Foarde, K.K. and Sparks, L.E. (1999). The Effect of Loading Dust Type on the Filtration Efficiency of Electrostatically-charged Filters. *Proceedings of Indoor Air '99*, Edinburgh, Scotland, August 8−13, 1999.

Hinds, W.C. (1999). *Aerosol Technology: Properties, Behaviour, and Measurement of Airborne Particles*, John Willey and Sons, New York.

Huang, S.H., Chen, C.W., Chang, C.P., Lai, C.Y. and Chen, C.C. (2007). Penetration of 4.5 nm and 10 μm Aerosol Particles through Fibrous Filters. *J. Aerosol Sci*. 38: 719–727.

Hussein, T., Glytsosc, T., Ondracek, J., Dohanyosova, P., Zdimald, V., Hameri, K., Lazaridis, M., Smolik, J. and Kulmala, M. (2006). Particle Size Characterization and Emission Rates during Indoor Activities in a House. *Atmos. Environ*. 40: 4285–4307.

Ji, J.H., Bae, B.N., Kang, S.H. and Hwang, J.H. (2003). Effect of Particle Loading on the Collection Performance of an Electret Cabin Air Filter for sSubmicron Aerosols. *J. Aerosol Sci*. 34: 1493–1504.

KACA (Korean Air Cleaning Association). (2007). *Air Cleaning Handbook - Volume 1*, Korean Air Cleaning Association, Seoul.

Kim, C. Noh, K.C. and Hwang, J. (2010). Numerical Investigation of Corona Plasma Region in Negative Wire-to-duct Corona Discharge. *Aerosol Air Qual. Res.* 10: 446–455.

Kim, K.H., Sekiguchi, K., Kudo, S., Sakamoto, K., Hata, M., Furuuchi, M., Otani, Y. and Tajima, N. (2010). Performance Test of an Inertial Fibrous Filter for Ultrafine Particle Collection and the Possible Sulfate Loss when Using an Aluminum Substrate with Ultrasonic Extraction of Ionic Compounds. *Aerosol Air Qual. Res*. 10: 616–624.

Kim, S.C., Harrington, M.S. and Pui, D.Y.H. (2007). Experimental Study of Nanoparticles Penetration through Commercial Filter Media. *J. Nanopart. Res*. 9: 117–125.

Kimura, N. and Iinoya, K. (1959). Experimental Studies on the Pressure Drop Characteristics of Fiber Mats. *Kagaku Kogaku*. 23: 792. (in Japanese)

Li, K. and Jo, Y.M. (2010). Dust Collection by a Fiber Bundle Electret Filter in an MVAC System. *Aerosol Sci. Technol*. 44: 578–587.

Liu, M., Claridge, D.E. and Deng, S. (2003). An Air Filter Pressure Loss Model for Fan Energy Calculation in Air Handling Units. *Int. J. Energy Res.* 27: 589–600.

Long, C.M., Suh, H.H., Catalano, P.J. Koutrakis, P. (2001). Using Time- and Size-Resolved Particulate Data to Quantify Indoor Penetration and Deposition Behavior. *Environ. Sci. Technol*. 35: 2089–2099.

Madl, A.K. and Pinkerton, K.E. (2009). Health Effects of Inhaled Engineered and Incidental Nanoparticles. *Crit. Rev. Toxicol*. 39: 629–658.

Nifuku, M., Zhou, Y., Kisiel, A., Kobayashi, T. and Katoh, H. (2001). Charging Characteristics for Electret Filter Materials. *J. Electrostat.* 51–52: 200–205.

Noh, K.C. and Hwang, J. (2010). The Effect of Ventilation Rate and Filter Performance on Indoor Particle Concentration and Fan Power. *Indoor Built Environ*. 19: 444–452.

Owen, M.K. and Ensor, D.S. (1990). Particle Size Distribution for an Office Aerosol. *Aerosol Sci. Technol*. 13: 486–492.

Podgórski, A. and Bałazy, A. (2008). Novel Formulae for Deposition Efficiency of Electrically Neutral, Submicron Aerosol Particles in Bipolarly Charged Fibrous Filters Derived Using Brownian Dynamics Approach. *Aerosol Sci. Technol*. 42: 123–133.

Romay, F.J., Liu, B.Y.H. and Chae, S.J. (1998). Experimental Study of Electrostatic Capture Mechanisms in Commercial Electret Filters. *Aerosol Sci. Technol*. 28: 224–234.

Shin, W.G., Mulholland, G.W., Kim, S.C. and Pui, D.Y.H. (2008). Experimental Study of Filtration Efficiency of Nanoparticles below 20 nm at Elevated Temperatures. *J. Aerosol Sci*. 39: 488–499.

Tabti, B., Dascalescu, L., Plopeanu, M., Antoniu, A. and Mekideche, M. (2009). Factors that Influence the Corona Charging of Fibrous Dielectric Materials. *J. Electrostat.* 67: 193–197.

Tekasakul, S., Suwanwong, P., Otani, Y. and Tekasakul, P. (2008). Pressure Drop Evolution of a Medium-Performance Fibrous Filter during Loading of Mist Aerosol Particles. *Aerosol Air Qual. Res.* 8: 348–365.

Zuraimi, M.S. and Tham, K.W. (2009). Reducing Particle Exposures in a Tropical Office Building Using Electrostatic Precipitators. *Build. Environ*. 44: 2475–2485.

Received for review, November 5, 2010
Accepted, December 27, 2010